

# Simple Stellar Population Models as probed by the Large Magellanic Cloud Star Cluster ESO 121–SC03

Y. Xin<sup>1,2,3\*</sup>, L. Deng<sup>2</sup>, R. de Grijs<sup>1,2</sup>, A. D. Mackey<sup>4</sup>, and Z. Han<sup>3</sup>

<sup>1</sup>*Department of Physics and Astronomy, The University of Sheffield, Hicks Building, Hounsfield Road, Sheffield S3 7RH*

<sup>2</sup>*National Astronomical Observatories, Chinese Academy of Sciences, Beijing 100012, P. R. China*

<sup>3</sup>*National Astronomical Observatories/Yunnan Observatory, Chinese Academy of Sciences, Kunming, Yunnan 650011, P. R. China*

<sup>4</sup>*Institute for Astronomy, University of Edinburgh, Royal Observatory, Blackford Hill, Edinburgh, EH9 3HJ*

Accepted —. Received —; in original form —

## ABSTRACT

The presence of blue straggler stars (BSs) in star clusters has proven a challenge to conventional simple stellar population (SSP) models. Conventional SSP models are based on the evolution theory of single stars. Meanwhile, the typical locations of BSs in the colour-magnitude diagram of a cluster are brighter and bluer than the main sequence turn-off point. Such loci cannot be predicted by single-star evolution theory. However, stars with such properties contribute significantly to the integrated light of the cluster. In this paper, we reconstruct the integrated properties of the Large Magellanic Cloud cluster ESO 121–SC03, the only cluster populating the well-known age gap in the cluster age distribution, based on a detailed exploration of the individual cluster stars, and with particular emphasis on the cluster’s BSs. We find that the integrated light properties of ESO 121–SC03 are dramatically modified by its BS component. The integrated spectral energy distribution (ISED) flux level is significantly enhanced toward shorter wavelengths, and all broad-band colours become bluer. When fitting the fully integrated ISED of this cluster based on conventional SSP models, the best-fitting values of age and metallicity are significantly underestimated compared to the true cluster parameters. The age underestimate is  $\sim 40$  per cent if we only include the BSs within the cluster’s half-light radius and  $\sim 60$  per cent if all BSs are included. The corresponding underestimates of the cluster’s metallicity are  $\sim 30$  and  $\sim 60$  per cent, respectively. The populous star clusters in the Magellanic Clouds are ideal objects to explore the potential importance of BSs for the integrated light properties of more distant unresolved star clusters in a statistically robust manner, since they cover a large range in age and metallicity.

**Key words:** blue stragglers – globular clusters: individual: ESO 121–SC03 – Magellanic Clouds – galaxies: star clusters.

## 1 INTRODUCTION

Even using improved observational technologies, the number of galaxies with resolved stellar contents is limited. Comparison of the observed integrated spectral properties with models of “simple” stellar populations (SSPs; single-age, single-metallicity stellar populations), i.e. using the so-called population synthesis technique, is therefore a practical approach to studying the formation and evolution processes in unresolved galaxies and their components. As the basic building blocks of the evolutionary population synthesis (EPS) method, conventional SSP models are generally constructed based on the evolution theory of single stars. (We specify the

conventional SSP models throughout this paper as the theoretical SSP models based on single-star evolution theory.) Thus far, accuracy assessments of the existing suites of conventional SSP models have not yet adequately considered a potentially significant problem revealed by observations of star clusters.

By assuming that all the original member stars within a cluster are born at the same time from the same progenitor molecular cloud, so that they have the same age and metallicity, star clusters are generally considered as the closest counterparts in the real world to idealised SSPs. The major differences between a star cluster and a conventional model SSP of the same age and metallicity can be illustrated by fitting the observed colour-magnitude diagram (CMD) of the cluster with a theoretical single-star isochrone. Most of the

\* E-mail: y.xin@sheffield.ac.uk

member stars can be well fitted by the isochrone in terms of their positions in the CMD. The number distributions along the isochrone can be retrieved via the adopted stellar initial mass function (IMF), and the number of low-mass member stars can be conserved in the presence of evaporation due to dynamical evolution. Then, the most prominent difference should be attributed to those member stars “straggling” away from the isochrone. Yellow and red stragglers (Protegies Zwart et al. 1997a,b) are not considered in the work, because they are comparatively rare and less luminous than blue stragglers (BSs). The underlopers and faint stars bluer than the main sequence (MS) are not bright enough to be important. Therefore, special attention has only been focussed on the BSs in our previous work (Deng et al. 1999; Xin & Deng 2005, hereafter XD05; Xin, Deng & Han 2007, hereafter XDH07), in view of their potential non-negligible influence on the integrated properties of star clusters.

BSs have been widely observed in stellar systems of all scales and complexities, as shown by, e.g. Ahumada & Lapasset (2007) for Galactic open clusters (OCs), Piotto et al. (2004) for Galactic globular clusters (GCs), Carney et al. (2005) for the Galactic field stellar population, Johnson et al. (1999) for Large Magellanic Cloud (LMC) clusters, Alcaino et al. (2003) for Small Magellanic Cloud (SMC) clusters, and Mapelli et al. (2007) for dwarf spheroidal galaxies. Considering their general locations in the CMD, i.e., brighter and bluer than the MS turn-off point, BSs are remarkably hotter than the most luminous “normal” MS stars. Typically for old Population I star clusters, when the red clump giants (RCGs) are populated instead of the blue horizontal branch (HB), BSs can significantly enhance the cluster’s integrated spectrum at ultraviolet (UV) and blue wavelengths – the modifications may lead to the star cluster being predicted as younger or of lower metallicity based on conventional SSP models, and therefore cause uncertainties when simply applying the conventional SSP models in EPS studies (XD05; XDH07). Meanwhile, the most likely formation mechanisms of BSs are all related to stellar interactions, including mass transfer in close binaries (e.g., Tian et al. 2006; and references therein) and stellar collisions in high-density regions (e.g., Sills et al. 2005; and references therein). This provides the theoretical support for this empirical work, since the consequences of the products of stellar interactions are not included in the conventional SSP models.

In order to empirically correct the conventional SSP models for the presence of luminous BSs, we construct the integrated spectrum of an SSP (i.e., a realistic star cluster) by analysing the individual stars, after careful consideration of their membership probability. We assume that the stellar population of a cluster is composed of two components: (i) all member stars that can be well fitted by a single-star isochrone represent a conventional SSP for the cluster’s real age and metallicity (e.g., SSP models from Bruzual & Charlot 2003; hereafter BC03); and (ii) BSs are responsible for the modifications to the conventional SSPs, and their contributions are considered by including the individual spectra of BSs. By combining these two components we may obtain a better approximation to the true SSP corresponding to the cluster of interest (see for details XD05 and XDH07).

In our previous work (XD05; XDH07), a sample of 100 Galactic OCs spanning an age range  $\in [0.1, 10]$  Gyr and a range in metallicity,  $Z \in [0.005, 0.035]$  (where solar metallic-

ity is  $Z_{\odot} = 0.020$ ), was used to detect BS contribution semi-empirically. The general results from our Galactic OC studies show that the integrated spectral properties of the sample clusters are dramatically modified by their BS components. A preliminary assessment of the uncertainties inherent to the conventional SSP models was made. Using either spectra or broad-band colours, the resulting ages and/or metallicities will be underestimated significantly: conservatively, the age underestimates are  $\sim 50$  per cent, as are the likely underestimates of the metallicity (although they are less accurately constrained because of our lower resolution in metallicity).

The results from the Galactic OCs clearly showed the non-negligible contributions of BSs to the integrated properties of SSPs. However, the numbers and distributions of BSs in OCs are affected by significant stochastic uncertainties (Ahumada & Lapasset 1995, 2007). To make the results and conclusions more reliable and convincing, we expand our working sample by including star clusters in the Magellanic Clouds (MCs). MC clusters hold significant advantages over Galactic OCs: (i) they span a wider range in both age and metallicity, and (ii) they are significantly more massive than their counterparts in the Galaxy, and therefore provide better statistics on an individual cluster basis (e.g., Mackey & Gilmore 2003a,b; de Grijs & Anders 2006).

In this paper, the LMC cluster ESO 121–SC03 is analyzed using its integrated spectral properties. This serves as the first example to detect BS contributions to the conventional SSP models using a massive intermediate-age cluster in a low-metallicity environment, based on a novel approach and better statistics than we were afforded by our use of Galactic OCs. ESO 121–SC03 ( $\alpha_{2000} = 06^{\text{h}}02^{\text{m}}01^{\text{s}}.36$ ,  $\delta_{2000} = -60^{\circ}31'22''.6$ ) is a distant northern LMC cluster, lying at a projected angular separation of  $\sim 10^{\circ}$  from the LMC centre. It is described as a “unique” LMC cluster by Mackey, Payne & Gilmore (2006; hereafter MPG06), because it is the only known cluster to lie in the LMC age gap. A significant number of previous studies (e.g., Mateo et al. 1986; Bica et al. 1998; MPG06) claim an absolute age of ESO 121–SC03 in the range of 8 – 10 Gyr. Mateo et al. (1986) obtained  $[\text{Fe}/\text{H}] = -0.9 \pm 0.2$  combined with a reddening of  $E(B - V) = 0.03$  mag. MPG06 derive  $[\text{Fe}/\text{H}] = -0.97 \pm 0.01$  and  $E(V - I) = 0.04 \pm 0.02$  for the cluster. MPG06 also mark a region in the CMD used to define BS candidates in the cluster, but they do not study the BS population in detail.

We present our photometric data reduction steps in Section 2. In the subsequent sections we present the details of the model construction and our main results. The CMD and the best-fitting isochrone of the cluster are discussed in Section 3. The identification of BSs in the CMD is described in Section 4. A discussion of the contributions of BSs to the integrated spectral properties of the cluster is presented in Section 5. In Section 6, the synthetic integrated spectral energy distribution (ISED) of the cluster is fitted with conventional SSP models in order to assess the uncertainties. Finally, a summary and the conclusions of this study are presented in Section 7.

## 2 DATA REDUCTION

We take advantage of the accurate photometric data taken with the Advanced Camera for Surveys (ACS) Wide Field

Channel (WFC) on board the *Hubble Space Telescope* (*HST*) as part of the *HST* Cycle 12 snapshot survey of MC star clusters (programme 9891, PI G. Gilmore). The ACS WFC consists of two  $2048 \times 4096$  pixel CCDs with a scale of  $\sim 0.05$  arcsec pixel $^{-1}$ , separated by a gap of  $\sim 50$  pixels, and approximately covers a field of view of  $202 \times 202$  arcsec $^2$ . The frame was taken in each of two filters, F555W and F814W. Exposure times were 300s and 200s, respectively. Further instrumental and observational details can be found in series of publications based on this programme, e.g., Mackey & Gilmore (2004), MPG06, and Mackey & Broby Nielsen (2007).

We retrieved the FITS files from the STScI data archive. The observations were reduced using the STScI reduction pipeline, i.e., they have had bias and dark current frames subtracted and are divided by flat-field images. The photometry was performed with the DOLPHOT software (Dolphin 2000), specifically the ACS module. Before we performed the photometry, we first prepared the images using the DOLPHOT tasks *acsmask* and *splitgroups*. These two packages mask out all bad pixels in the images and then split the multi-image STScI FITS files into a single FITS file per chip, respectively. We then used the main DOLPHOT routine to make photometric measurements on the pre-processed images, using the F814W drizzled frame as the position reference. All running parameters were set to the recommended values in the DOLPHOT manual. The output photometry was obtained in the VEGAMAG system and corrected for charge-transfer efficiency degradation. Photometric calibrations and transformations were done following Sirianni et al. (2005).

To obtain a high-quality CMD of the cluster, we used three parameters from DOLPHOT to filter the photometric results. The “sharpness” measures how broad the intensity profile of a detected object is relative to the point-spread function (PSF). It is zero for a perfectly fit star, positive for an object that is too sharp (i.e., perhaps a cosmic ray), and negative for an object that is too broad (i.e., perhaps a blend, cluster, or background galaxy). The “crowding” parameter is given in magnitudes, and measures how much brighter the object would have been measured had nearby objects not been fit simultaneously. For an isolated star the “crowding” value is zero. The  $\chi^2$  parameter represents the quality of the PSF fitting. In this paper, we selected only objects with  $-0.3 \leq \text{sharpness} \leq 0.3$ ,  $\text{crowding} \leq 0.5$  mag, and  $\chi^2 \leq 0.25$  in both frames. Meanwhile, we only kept objects classified as good star (object type 1) and star errors of types 1–7 by DOLPHOT, which are referred to as “usable” in the DOLPHOT manual.

After following through this procedure, 2824 objects were detected in the field of ESO 121-SC03. In order to evaluate the completeness of the data, DOLPHOT was employed again, in artificial-star mode. We generated  $\sim 10^6$  fake stars, which were created with the DOLPHOT task *acsfakelist*. The limits of the artificial stars were set to 16.0–28.0 mag in magnitudes and  $-0.50 - 2.00$  mag in colours in the CMD. The fake stars were binned in four-dimensional space: 200 pixels in  $x$ - and  $y$ - positions, respectively, 0.2 mag in brightness and 0.25 mag in colour. The completeness function of the cluster is shown in Fig. 1, integrated over position and colour, as a function of  $m_{F555W}$ . Completeness declines

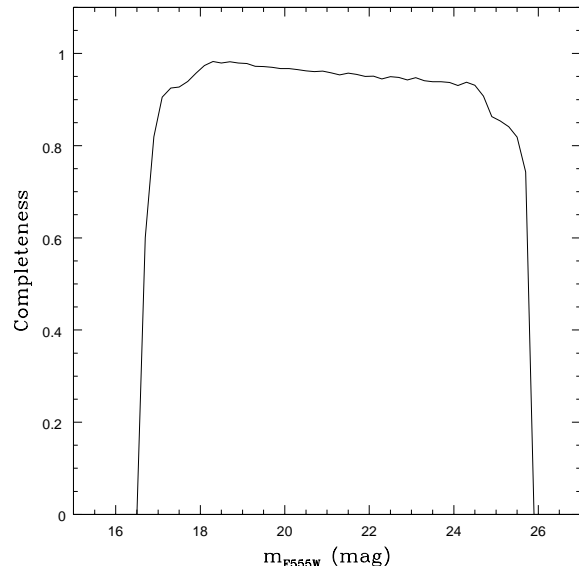


**Figure 1.** Completeness function of ESO 121-SC03. The function has been integrated over position and colour as a function of  $m_{F555W}$ .

for  $m_{F555W} \leq 18$  mag because we do not have any stars of that brightness in the CMD.

### 3 COLOUR-MAGNITUDE DIAGRAM

The final, cleaned CMD of ESO 121-SC03 in  $m_{F555W}$  and  $m_{F814W}$  magnitudes is presented in Fig. 2. It is clearly shown that the CMD is well defined and contains little field contamination. The perfectly represented evolutionary stages, e.g., MS, red-giant branch (RGB), and RCG, indicate the high accuracy of the photometry and the validity of the reduction procedure. The CMD reaches more than 3 magnitudes below the Main sequence turn-off (MSTO). All these aspects help us to perform a detailed and highly accurate statistical study of the cluster.

As described in Section 1, the synthetic ISED of a cluster is constructed by assuming that the entire stellar population of the cluster can be decomposed into two components: one accounts for all member stars that are well fitted by a given isochrone (of single stars) for the appropriate cluster age and metallicity; the other includes only the cluster’s BS population, which is therefore referred to as the BS component. All other member stars deviating from the fitted isochrone can be neglected because of their low luminosity and relatively small number. More details justifying this approach can be found in XD05.

To follow the same procedure for ESO 121-SC03, we first need to find the isochrone that best matches the observed features of the cluster’s CMD, and use this to derive accurate physical parameters, including the cluster’s age, metallicity, colour excess and distance modulus. These parameters are very important for our construction of the ISED of the SSP component and for defining the BS population. The photometry in the VEGAMAG system is transformed into Johnson-Cousins  $V$  and  $I$  magnitudes following

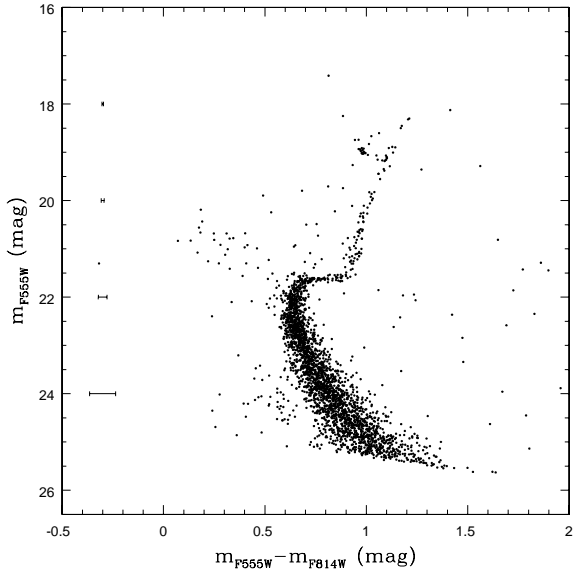


**Figure 2.** Cleaned CMD of ESO 121-SC03. The CMD contains 2824 detections. The photometric data is plotted in the VEGA-MAG system.

the prescription of Sirianni et al. (2005), and subsequently the new CMD in  $V, (V - I)$  is used to find the best-fitting isochrone. The fit quality and corresponding details are displayed in Fig. 3.

As the first step to identify the best-fitting isochrone, we attempted to identify the MSTO in the CMD by counting the number of stars in bins of magnitude (0.01 mag) and colour (0.001 mag) in the turn-off region; the intersection of two bins with maximum stellar numbers, one in magnitude and the other in colour, is regarded as the cluster’s MSTO. The resulting MSTO locus is at  $(V - I)_{\text{TO}} = 0.606 \pm 0.005$  mag and  $V_{\text{TO}} = 21.94 \pm 0.01$  mag. Next, the same procedure is adopted to identify the main sequence ridge line (MSRL) in the CMD: the numbers of stars are measured in magnitude bins of 0.5 mag, from the MSTO to 3 magnitudes below the MSTO. In Fig. 3, the calculated MSTO is marked as the solid bullet, and the MSRL is marked by solid triangles.

We used the Padova2000 theoretical isochrones (Girardi et al. 2000) to fit the observed CMD. The original Padova2000 isochrones were interpolated to  $[\text{Fe}/\text{H}] = -0.97$  dex (the value given by MPG06). In total nine points, including the six MSRL points, the bottom of the RGB, the mean location of the RCG, and the point on the RGB at the level of the intermediate magnitude between the points of the RGB bottom and the mean RCG locus, were used as fiducial points to evaluate the fit quality. Next, we calculated the standard deviation ( $\sigma$ ) for the offsets between the nine fiducial points in the CMD and the isochrone, in order to obtain the minimum  $\sigma$  value. The isochrone fitting also offered us estimates for the apparent distance modulus,  $(m - M)_V$ , and the foreground extinction suffered by the cluster.

Given the above results and discussion, we adopted the metallicity of  $[\text{Fe}/\text{H}] = -0.97$  dex, and we found a best-fitting isochrone of age =  $8.9_{-0.3}^{+1.1}$  Gyr, with  $(m - M)_V =$

$18.30 \pm 0.06$  mag and  $E(V - I) = 0.03 \pm 0.01$  mag. These values will be used in the remainder of this paper.

Our measurements for ESO 121-SC03 are in good agreement with previous results. We derived that the age of the cluster is  $8.9_{-0.3}^{+1.1}$  Gyr, which is entirely consistent with the age estimates of MPG06, who provided an age range of 8.3 – 9.8 Gyr for ESO 121-SC03. Similarly, Mateo et al. (1986) found that this cluster is  $10 \pm 2$  Gyr or  $8 \pm 2$  Gyr old if the LMC distance modulus is 18.2 or 18.7 mag, respectively. Bica et al. (1998) gave an age of 8.5 Gyr for the cluster from Washington photometry. Besides the similar age value, our result confirm the conclusion of MPG06 and Mateo et al. (1986) that ESO 121-SC03 is the only known cluster lying within the LMC age gap. The LMC has a unique cluster formation history where nearly all of its star clusters were formed either  $\sim 13$  Gyr ago or less than  $\sim 3$  Gyr ago (Da Costa 1991; Geisler et al. 1997 and references therein; see also Parmentier & de Grijs 2007). As suggested by numerical simulations (e.g., Bekki et al. 2004), the origin of the age gap is associated with the dynamical interaction between the LMC and the SMC about 3 – 4 Gyr ago. However, no theoretical studies have explained the existence of ESO 121-SC03. Bica et al. (1998) considered that this cluster may have originated from a recent accretion of dwarf galaxies, but Dirsch et al. (2000) concluded that the accretion of ESO 121-SC03 is not necessary, since they found that this cluster has a similar age-metallicity relation as the LMC field stars. In this respect, ESO 121-SC03 may reveal important information about the formation and evolution history of the LMC.

The  $(m - M)_V$  and  $E(V - I)$  values for ESO 121-SC03 were determined based on the offsets in, respectively, magnitude and colour required to align the MSTO of the isochrone with that of the observed CMD. Thus, it is worth considering the consistency between our results and those from other work based on different methods. There are few estimates of the colour excess for ESO 121-SC03. Both Mateo et al. (1986) and Bica et al. (1998) adopted  $E(B - V) = 0.03$  mag from the Burstein & Heiles (1982) maps, which approximates to  $E(V - I) \sim 0.04$  mag via the empirical relation  $E(V - I) = 1.31E(B - V)$  (e.g., Mackey & Gilmore 2003a,b). MPG06 obtained metallicity and reddening values of  $[\text{Fe}/\text{H}] = -0.97 \pm 0.10$  dex and  $E(V - I) = 0.04 \pm 0.02$  mag using the method of Sarajedini (1994). All of these values are consistent with our isochrone-fitting result of  $E(V - I) = 0.03 \pm 0.01$  mag (using  $[\text{Fe}/\text{H}] = -0.97$  dex), which proves that there are no significant errors in our photometric transformation from the ACS/WFC system to the Johnson-Cousins  $V$  and  $I$  system.

We obtained  $(m - M)_V = 18.30 \pm 0.06$  mag in this paper, which is larger than the value from MPG06 ( $18.11 \pm 0.09$  mag) and smaller than the standard LMC distance modulus ( $18.50 \pm 0.09$  mag, see e.g., Gratton et al. 2003). In terms of the linear distance, ESO 121-SC03 in our work is  $\sim 10$  per cent closer to us than the centre of the LMC, but  $\sim 10$  per cent more distant than suggested by the distance modulus of MPG06. Adopting the optical centre of the LMC at  $\alpha = 05^{\text{h}}20^{\text{m}}56^{\text{s}}$  and  $\delta = -69^{\circ}28'41''$  (Bica et al. 1996), ESO 121-SC03 lies at a projected angular separation of  $\sim 10^{\circ}$ . Adopting the distance modulus in our work, the linear distance between the centre of the LMC and ESO 121-SC03 is  $\sim 9.5$  kpc. This value is smaller than that in MPG06 (11.5

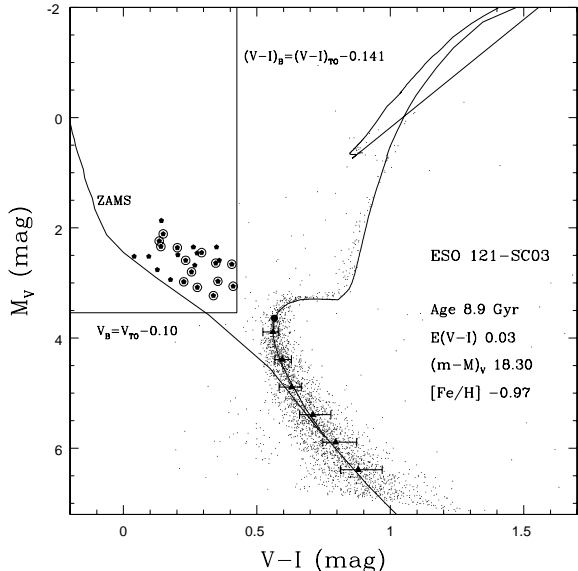


**Figure 3.** Cleaned CMD for ESO 121-SC03. The photometry has been transformed from the VEGAMAG system to Johnson-Cousins  $V$  and  $I$  magnitudes. The best-fitting Padova2000 isochrone is overplotted. The corresponding fit parameters are included in the figure legend. In the CMD, we define a region that we will use for the identification of the cluster’s BS population. The ZAMS is the Padova1994 isochrone at  $\log(\text{age yr}^{-1}) = 6.60$  and  $[\text{Fe}/\text{H}] = -0.97$  dex. The solid bullet is the cluster’s MSTO. The solid triangles represent the MSRL of the cluster. Pentagons are blue stragglers. See the text (Sections 3 and 4) for details.

kpc), but still agrees with the conclusion in MPG06 that ESO 121-SC03 is one of the most remote known LMC star clusters.

#### 4 THE BLUE STRAGGLER POPULATION

As shown in Fig. 3, ESO 121-SC03 is a “clean” cluster and includes an obvious population of BS candidates, which is very advantageous for our main aim of analysing the BS contributions to the ISED of the cluster. However, we still need to be very careful in the selection of BS members, since we do not have access to classical membership probability assessment methods (i.e., proper motions and/or radial velocities) that can reliably remove field stars from the CMD. In this paper, we will try to reduce as much as possible any contamination to the BS population of the cluster due to field stars and improper classifications due to possible member stars in the MSTO region. Two measurements were adopted to avoid exaggerating the BS population in the cluster.

First, to properly account for the photometric and systematic errors, we defined a BS region in the CMD using three boundary limits:  $V_B$ ,  $(V-I)_B$ , and the theoretical ZAMS, as shown in Fig. 3,

$$\begin{aligned} V_B &= V_{\text{TO}} - 0.10 & \text{and} \\ (V-I)_B &= (V-I)_{\text{TO}} - 0.141 \end{aligned} \quad (1)$$

The offset of 0.10 mag in  $V_B$  relative to the MSTO of

the cluster was adopted as an empirical estimate of the photometric and systematic errors for *HST*/ACS WFC observations (Sirianni et al. 2005); the offset of 0.141 mag in  $(V-I)_B$  was obtained similarly.

The theoretical ZAMS is represented by the MS ridge line of the youngest isochrone ( $\log(\text{age yr}^{-1}) = 6.60$ ) in the Padova1994 library (Bertelli et al. 1994). We have taken this approach mainly because there is no such an isochrone in the Padova2000 library: the updated equation of state adopted in Padova2000 is only sensitive to the evolution of stars with initial masses from 0.15 to 7  $M_{\odot}$  (Girardi et al. 2000). Therefore, the age coverage is  $\log(\text{age yr}^{-1}) = [7.80, 10.25]$  in Padova2000 (a 7  $M_{\odot}$  star is still on the MS at  $\log(\text{age yr}^{-1}) = 6.60$ ). Meanwhile, the youngest isochrone fully matches the requirement for a ZAMS in this paper, where it serves as one of the boundaries for the identification of BSs. The ZAMS is not involved in fitting the BS positions in the CMD – for the fitting we use only the Padova2000 isochrones.

Secondly, the obvious central concentration of BSs has been widely observed in stellar systems (e.g., Lee et al. 2003 for the Sextans dwarf spheroidal galaxy; Ferraro et al. 2003 for GCs). Meanwhile, the radial distributions of BSs are observed to be bimodal in some clusters (i.e., strongly peaked in the cluster centre, decreasing at intermediate radii and rising again at greater distances), as shown by, e.g., Ferraro et al. (1997) for M3, Ferraro et al. (2004) for 47 Tuc, Sabbi et al. (2004) for NGC 6752, and Warren et al. (2006) for M5. This behaviour has been suggested as probably due to the relative efficiency of two major BS formation mechanisms: the mass-transfer scenario should mainly populate the BS population in the lower-density outskirts of GCs, and the collisional scenario is the most probable formation mechanism in the high-density inner regions (e.g., Lanzoni et al. 2007; and references therein).

Since there are no membership probability measurements available for our cluster, the BSs identified by their loci in the CMD are all considered as BS member candidates, and they are divided into two cases in this paper: (i) BSs inside the half-light radius ( $R_{\text{HL}}$ ) of the cluster. This provides a conservative estimate of the BS contribution to the total light of the cluster, and these BSs are marked with open circles in Fig. 3; (ii) all BSs in the cluster (pentagons in Fig. 3 and solid circles in Fig. 4). This brackets the maximum alteration to the conventional SSP model for the cluster due to BSs. There are 14 BSs in case (i) among a total of 25 BSs in case (ii).

Incompleteness corrections were taken into account for the identification of both the BS population and the cluster’s  $R_{\text{HL}}$ . Comparing the BS selection box in Fig. 3 with the incompleteness function in Fig. 1, we found that the level of incompleteness was not significant at the luminosity level of the BSs. The integrated correction for the number of the entire BS population is only one BS, but one bright and/or blue BS may cause a significant difference to the modification of the integrated spectral properties of the cluster. Therefore, instead of taking the risk of putting an artificial BS somewhere in the BS region, we decided to keep using the observed BS candidates, and we assumed that the full sample of BS candidates detected in the cluster corresponded to its entire BS population. After the incompleteness correc-

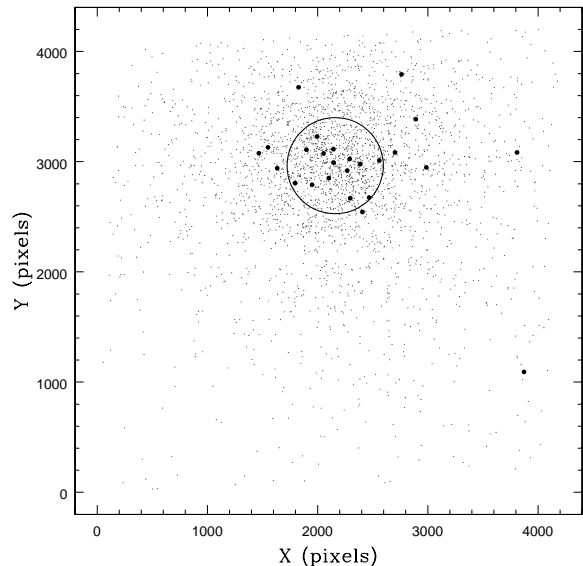


**Figure 4.** Pixel coordinates of all 2824 detected stars in ESO 121-SC03. The large circle marks the cluster’s half-light radius ( $R_{\text{HL}} = 21.8$  arcsec). The solid circles are the BSs.

tion, we derived the cluster’s  $R_{\text{HL}}$ ,  $R_{\text{HL}} = 21.8 \pm 1.0$  arcsec, shown as a large circle in Fig. 4.

## 5 MODIFICATIONS TO THE INTEGRATED SPECTRAL PROPERTIES

### 5.1 SSP model reconstruction – the synthetic ISED

The synthetic ISED of the cluster including the BS contribution was constructed by assuming that the stellar population of the cluster is made up of two components, i.e., an SSP component and a BS component. The ISEDs of these two components were derived separately, and the summation of the ISEDs of these two components gives the new ISED of the cluster. The resulting synthetic ISED is then treated as the ISED of the true SSP corresponding to the parameters of the cluster. The contributions to the ISED of the cluster due to BSs are measured by comparing the integrated properties between the conventional ISED (i.e., the ISED of the SSP component) and the synthetic ISED.

To build the ISED of the BS component, the spectrum of each single BS must be derived from the observed photometric data. To this end, we used Padova2000 isochrones of the same metallicity but younger ages than the cluster’s SSP to match the locus in the CMD of each BS individually. The parameters of effective temperature ( $T_{\text{eff}}$ ) and surface gravity ( $\log g$ ) (roughly equivalent to luminosity and mass) for each BS can be determined by interpolating between the two closest isochrones representative of the BS. Based on the  $T_{\text{eff}}$  and  $\log g$  determined in this way, a theoretical spectrum from the stellar spectral library of Lejeune et al. (1997) was assigned to the BS. The theoretical spectra were also interpolated, so that the same metallicity as that of the cluster was adopted. This process was performed individually for all BSs in the cluster, and the ISED of the BS component

is given by adding up the individual spectra of the BSs directly.

$$F_{\text{BS}} = \sum_{i=1}^{N_{\text{BS}}} f_{\text{BS}}^i \quad , \quad (2)$$

A significant amount of theoretical work has focused on BS formation models. BSs from equal-mass MS star collisions (Benz & Hills 1987) may suffer from huge mass loss and undergo complete chemical composition mixing – the unclear clock will, in effect, be reset to a ZAMS star. Unequal-mass MS star collisions (Benz & Hills 1992) may cause much less mass loss, but also violent mixing in the atmosphere of the more massive star – this may revert the observational parameters of the more massive star back to those of a helium-rich MS star. Meanwhile, Lombardi et al. (1995, 2002) argued that BSs from stellar collisions would not be expected to have either a significant helium enhancement in the outer envelope, nor replenished fresh hydrogen fuel in their cores. Detailed spectral analysis of BSs and turn-off region MS stars in M67 (e.g., Mathys 1991; Shetrone & Sandquist 2000) led to the conclusion that the Fe and Ca abundances of BSs are very close to those of the MS stars in the cluster. Liu et al. (in prep.) conclude that most BSs exhibit similar properties to those of regular MS stars, based on a detailed analysis of low-resolution spectra of all BSs in M67.

It is clear that rotational support and the stellar chemical profile are very important, because they have profound effects on stellar evolution and on the remnant’s position in a CMD (Sills et al. 2000), to which our method of obtaining the BS spectrum is certainly sensitive. However, until either a well-established theory emerges that can predict the actual internal structure of all BSs in a CMD, or high-resolution spectra are available for all BSs in a CMD, the theoretical approaches followed in this series of papers (XD05, XDH07, and the present paper) are fully adequate, as long as we restrict ourselves to low-resolution spectroscopic analysis.

The main goal of this series of papers is to remedy the conventional SSP models empirically by analyzing the contributions of the observed BSs quantitatively. To reach this goal, what is really needed is a quantification of the relative modifications to conventional SSP models when the same basic ingredients (i.e., isochrone library, spectral library, and IMF) are used to describe both the conventional SSP and the BS contribution. As discussed in the previous sections, the positions of BSs in the observed CMD are fitted with Padova2000 isochrones, and the BS spectra are extracted from the Lejeune et al. (1997) stellar spectral library. Therefore, the conventional SSP models (BC03) based on the same libraries and using a Salpeter (1955) IMF are adopted to represent the properties of the SSP components in star clusters. We interpolated the ISEDs across a grid of age and metallicity to construct the ISED of the SSP component so that they match the parameters of the cluster.

For an SSP of age  $t$  and metallicity  $Z$ , assuming an IMF  $\phi(m)$ , the ISED of the SSP component is

$$F_{\text{SSP}}(\lambda, t, Z) = A \int_{m_l}^{m_u} \phi(m) f(\lambda, m, t, Z) dm \quad , \quad (3)$$

where  $f(\lambda, m, t, Z)$  is the flux of a single star of mass  $m$ , age  $t$ , and metallicity  $Z$ ;  $m_u$  and  $m_l$  are the upper and lower

integration limits in mass, respectively.  $A$  is a normalization constant, which is used to restore the flux of the SSP component to its real intensity.

The ISEDs of BC03 SSP models are all normalized to a total mass of  $1 M_{\odot}$  in stars, at  $t = 0$ . Therefore, we need to calibrate the ISEDs of the BS and SSP components similarly. In order to do so, we count the number of stars in the CMD in the magnitude interval between the MSTO and the point at two magnitudes below the MSTO on the MS. This number is defined as  $N_2$  (Ahumada & Lapasset 1995).  $N_2$  is used to calculate the normalization constant  $A$  in Eq. (3). By using a Salpeter IMF,  $A$  can be derived as follows:

$$N = A \int_{m_1}^{m_2} m^{-2.35} dm = N_2 \quad , \quad (4)$$

where  $m_2$  and  $m_1$  are, respectively, the stellar masses at the MSTO and at the point 2 magnitudes below the MSTO. To ensure the integrity of the stellar number counts in this range, the photometry should be sufficiently deep. The photometric observational data used in this paper meets this requirement. Corrections for incompleteness in this mass range are also applied. For a detailed description of the model construction procedure, see XD05 and XDH07.

Incidentally, the choice of the IMF also introduces uncertainties in the SSP's integrated properties, but it is unimportant for the discussion in this series of papers. The conventional SSP models using a Salpeter IMF are only used as a reference to the ISEDs of the SSP components, what is really important in the current context is the contributions of BSs to the ISED; the properties of the BSs in our cluster are determined individually, and independently of the adopted IMF properties.

## 5.2 Modification to the ISED

According to their loci in the CMD (Fig. 3), BSs are the bluest cluster members, with extraordinary luminosities, and thus they may cause very significant modifications to the conventional view of the integrated spectral properties of a cluster. The contributions of BSs to a cluster's ISED are demonstrated in Fig. 5 for two cases: (i) considering only the BSs inside  $R_{HL}$ ; and (ii) all BSs in the cluster.

In Fig. 5, the solid line is the ISED of the conventional SSP model with an isochrone-fitted (regarded as “true”) age and metallicity representative of that of the cluster, i.e., the ISED of the SSP component. The thin dotted line is the ISED of the BS component for case (i); the thin dashed line is the ISED of the BS component for case (ii). The heavy dotted line is the synthetic ISED of the SSP component and the case-(i) BS component; the heavy dashed line is the synthetic ISED of the SSP component and the case-(ii) BS component. Although they are not dominated by BSs, both synthetic ISEDs show significant enhancements across a wide range of UV, blue and visual wavelengths. The synthetic ISEDs become undoubtedly hotter than the ISED of the conventional SSP (solid line in Fig. 5). Taking the values of the flux at  $5510 \text{ \AA}$  as an example, the energy enhancements will be, respectively,  $\sim 10$  and  $\sim 18$  per cent if we include the case-(i) and case-(ii) BS components.

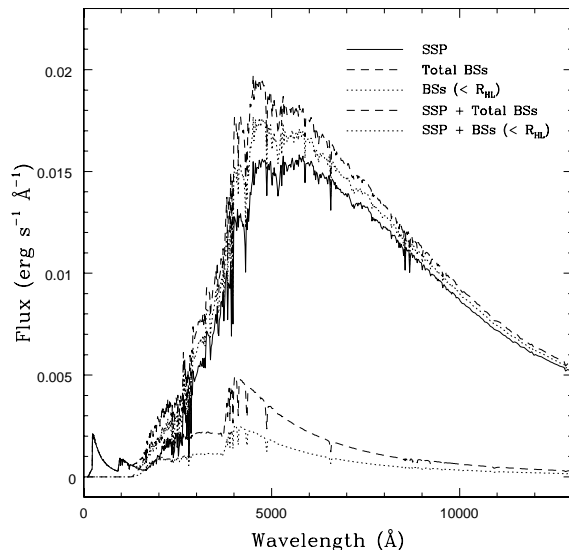


**Figure 5.** ISED modifications. The BS contributions are presented for two cases. The solid line is the ISED of the SSP component. The thin dotted line is the ISED of the BS component for case (i): BSs within  $R_{HL}$ . The thin dashed line is the ISED of the BS component for case (ii): all BSs in the cluster. The heavy dotted line is the synthetic ISED of the SSP component and the case-(i) BS component. The heavy dashed line is the synthetic ISED of the SSP component and the case-(ii) BS component.

## 5.3 Modification to the broad-band colours

This series of papers (this paper, XD05, and XDH07) has indicated that BSs in general stellar populations should be recognized and treated with special care when dealing with EPS studies of galaxies.

In addition to direct ISED analysis and spectral-index applications, photometric observations using broad-band filters are more frequently used than spectrophotometry when trying to understand stellar populations in distant and therefore often very faint galaxies. As shown in Fig. 5, the BS component enhances the ISED of the conventional SSP across a wide range of wavelengths, especially in the UV and blue. This tends to make the stellar population appear younger and/or more metal poor according to conventional SSP models, since both modifications can make the colours bluer.

Four broad-band colours,  $(U - B)$ ,  $(B - V)$ ,  $(V - R)$ , and  $(V - I)$ , are taken as probes in this paper to quantitatively measure the BS contributions for ESO 121-SC03. The colours are obtained by convolving the ISEDs with the corresponding filter response curves. The results are listed in Table 1. The colours on the first line are from the ISED of the cluster's SSP component, those on the second line are from the synthetic ISED of the SSP and the case-(i) BS component, and those on the third line are from the synthetic ISED of the SSP and the case-(ii) BS component. Based on the results in Table 1, we conclude that the broad-band colours are all modified, to some extent, with respect to the conventional models (line 1) owing to the presence of BSs. The influence of the BSs becomes more pronounced toward bluer wavelengths. For  $(U - B)$ , the colour modifica-

**Table 1.** The broad-band colours of the cluster for different cases.

Component	$(U - B)$ (mag)	$(B - V)$ (mag)	$(V - R)$ (mag)	$(V - I)$ (mag)
SSP	0.101	0.744	0.516	0.993
SSP + BSs $\leq R_{\text{HL}}$	0.091	0.683	0.487	0.945
SSP + all BSs	0.045	0.635	0.453	0.905

tion can be up to  $\sim 50$  per cent. For  $(B - V)$  and  $(V - R)$ , the modifications are  $\sim 10$  per cent. Even for  $(V - I)$ , our reddest colour, the changes are still more than 5 per cent. Although these modifications are specific to the case of ESO 121-SC03, i.e., for  $[\text{Fe}/\text{H}] = -0.97$  dex and an age of 8.9 Gyr, this example serves as a warning for the more general use of broad-band colours to derive cluster ages and metallicities based on theoretical SSP modeling.

Based on the modifications to the ISED and the broad-band colours calculated as examples in this paper, which are much greater than the observational errors, we strongly caution that conventional SSP models should be used carefully in evolutionary population synthesis of galaxies, at least for the intermediate and old population-I stars. It is difficult to trace the BS population in very young star clusters, and the old population-II star clusters usually have very extended HBs which, instead of the BSs, will dominate the integrated light at blue wavelengths.

## 6 UNDERESTIMATES OF AGES AND/OR METALLICITIES BY THE CONVENTIONAL SSP MODELS

In the previous section we showed that the ISED and broad-band colours of conventional SSPs (for the case of ESO 121-SC03) are modified dramatically by BS components, and the modifications will introduce sizeable uncertainties if conventional SSP models are used to obtain the basic physical parameters of a stellar population. Again, taking ESO 121-SC03 as an example, we try to quantify the uncertainties by fitting the synthetic ISED of the cluster using conventional SSP models. We focus on the age and metallicity, the two most important parameters of a stellar population.

As presented in Fig. 5, one of the main effects of BSs is to make the synthetic ISED hotter with respect to that of the conventional models, i.e., the spectra get enhanced more significantly towards shorter wavelengths. Technically, this hotter ISED can still be well fitted (or, say, misunderstood) by conventional SSP models of either younger age or lower metallicity, since both options make the ISED hotter. Therefore, we regard the synthetic ISED of ESO 121-SC03 as the real ISED (i.e., the ISED that will be observed spectroscopically), and we fit it with an ISED of a conventional SSP model. The standard deviation ( $\sigma$ ) is used to identify the best-fitting result. The differences between the real cluster parameters and the best-fitting results are used to discuss the uncertainties that intrinsically exist in the application of the EPS method.

We emphasize here that instead of building the actual ISED of a specific cluster, what we are really interested in is to discuss the potential uncertainties introduced when the BS component is completely ignored. Thus, although the

synthetic ISED is not exactly the real ISED of the cluster, the method and corresponding results are effective approaches to the problem.

### 6.1 Uncertainties in age

Fig. 6 shows the uncertainties in age: we fit the synthetic cluster ISED with the conventional SSP models, keeping the metallicity fixed while lowering the age values. The left-hand panel shows the results for the synthetic ISED of the SSP component plus the case-(ii) BS component (all BSs); the right-hand panel is the same but for the SSP component plus the case-(i) BS component (BSs within  $R_{\text{HL}}$ ). In the top panels, the solid line is the synthetic cluster ISED, the dotted line is the best-fitting ISED based on conventional SSP models, and the dashed line is the ISED of the SSP component. Plotting the SSP component's ISED in the figure is done to show the differences between the real ISED and the conventional model ISED with the true parameters, and to show that the SSP component's ISED does not correctly represent the observations. The conventional ISEDs are normalized to the real ISED at a wavelength of 5500 Å. In the bottom panels, the residuals between the synthetic ISED and the ISEDs of two conventional SSPs and the  $3\sigma$  regions are shown, respectively, using matching line styles.

Based on the results shown in Fig. 6 and assuming that the observed ISED is the only data available for stellar population analysis, the fitting with the conventional SSP models will result in a best-fitting age of 3.4 Gyr, which is more than 60 per cent younger than the real age of the cluster, 8.9 Gyr, determined from isochrone fits to the CMD; even considering only the BSs within  $R_{\text{HL}}$ , the best-fitting age of 5.4 Gyr still suffers from a non-negligible difference of  $\sim 40$  per cent. In the bottom panels, the  $\sigma$  values are indeed small for all cases – approximately at the level of only one per cent of the cluster's flux, but the  $\sigma$  value according to the best-fitting conventional ISED is always  $\sim \frac{2}{3} - \frac{3}{4}$  smaller than that from the SSP component of the cluster alone, which implies that the EPS method will probably lead to an incorrect best-fitting age in unresolved conditions.

### 6.2 Uncertainties in metallicity

In a similar way as in the previous section, Fig. 7 shows the uncertainties in metallicity in evolutionary population synthesis using the conventional SSP models. The meaning of the symbols and line styles in this figure is similar to that in Fig. 6. The results are also similar: the metallicities (expressed in  $[\text{Fe}/\text{H}]$ ) are significantly underestimated (i.e., more metal poor) as derived from the conventional SSP models. The underestimates will be  $\sim 60$  and  $\sim 30$  per cent, respectively, if we include the cases (ii) and (i) BS components. The detailed results are listed in Table 2. Taking the modifications in age as an example, the fit uncertainty is calculated as

$$\Delta_{\text{fit}} = \frac{(\text{age})_{\text{real}} - (\text{age})_{\text{fit}}}{(\text{age})_{\text{real}}}. \quad (5)$$

As shown in Figs. 6 and 7, the conventional SSP models can fit perfectly most of the features of the observed ISED, if we leave the parameters free. However, such good fits do not mean that we have obtained good determinations of the real



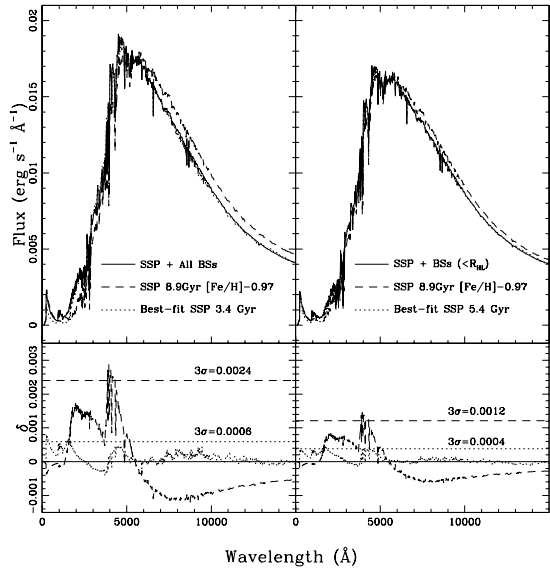


**Figure 6.** Fits of the synthetic ISED of ESO 121–SC03 with conventional SSP models – uncertainties in the age determination. The left-hand panel is for the synthetic ISED of the SSP component and all BSs. The right-hand panel is for the synthetic ISED of the SSP component and the BSs inside  $R_{\text{HL}}$ . In the top panels, the solid line is the synthetic cluster ISED (real ISED), the dotted line is the best-fitting ISED based on the conventional SSP models, and the dashed line is the ISED of the SSP component. The model ISEDs are normalised to the real ISED at a wavelength of 5500 Å. In the bottom panels, the differences between the synthetic ISED and the ISEDs of two conventional SSPs and the  $3\sigma$  regions are shown, respectively, using matching line styles.

physical parameters in unresolved conditions. Applications of conventional SSP models in EPS studies may therefore seriously suffer from the uncertainties addressed in this paper. This is true at least for the stellar populations corresponding to the star clusters that we have thus far analyzed.

## 7 SUMMARY AND CONCLUSIONS

In this paper, the LMC star cluster ESO 121–SC03 is taken as a specific cluster to show in detail the technique and procedure we have developed to assess the potential importance of BSs to the integrated properties of unresolved star clusters: data reduction, isochrone fitting, identification of the BS population, synthetic ISED construction, and the concept of detecting BS contributions to conventional SSP models using integrated light properties.

We construct the synthetic ISED of the cluster by decomposing the stellar population of the cluster into two components: the SSP component composed of all the member stars that can be well fitted by an isochrone of single stars; and the BS component defined by the BSs in the cluster. The synthetic ISED of the sum of these two components is regarded as the real ISED of the cluster. The contributions to the ISED of the cluster owing to the BS component are considered for two cases. For case (i), only BSs inside  $R_{\text{HL}}$  are used, which provides a conservative estimate of the modification caused by the presence of BSs; while for case (ii), all

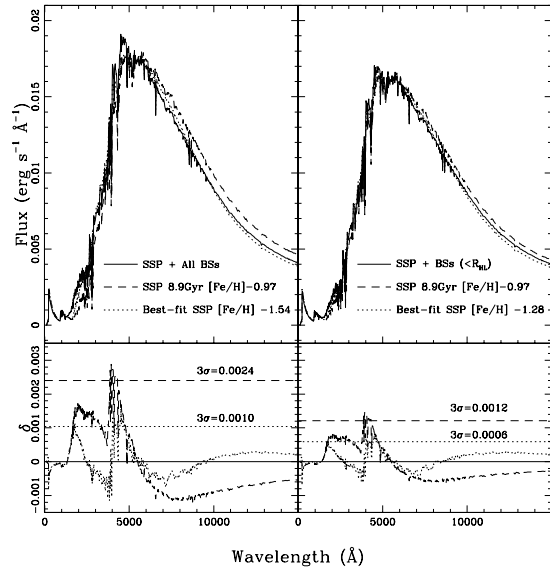


**Figure 7.** Fits of the synthetic ISED of ESO 121–SC03 with conventional SSP models – uncertainties in the metallicity determination. Figure coding is as for Fig. 6.

BSs in the cluster are included, which renders the maximum likely alteration to the conventional results. These two cases bracket a range of changes to the conventional SSP models caused by the BS population in a real cluster.

Integrated spectral properties are used to measure the modifications to the conventional SSP due to BSs. By the inclusion of BSs, the synthetic ISED of ESO 121–SC03 is greatly enhanced toward shorter wavelengths, and all UV and optical broad-band colours become bluer. Both of these observations can make the population appear a lot younger or more metal poor than would be derived from fitting conventional SSP models. The modifications are quantified by fitting the synthetic ISED with conventional SSP models. For the synthetic cluster ISED including only BSs inside  $R_{\text{HL}}$ , the age underestimate is at the level of  $\sim 40$  per cent, and the metallicity underestimate is  $\sim 30$  per cent. For the synthetic ISED that includes all BSs identified in the cluster, the underestimates of both age and metallicity increase to  $\sim 60$  per cent.

In view of the common occurrence of BSs in MC star clusters (e.g., Johnson et al. 1999; Alcaino et al. 2003), and given that our results for the comparatively rich MC clusters (at least, with respect to the Galactic OCs) are statistically robust, we have reason to believe that the BS effect discussed in this paper for ESO 121–SC03 may not be an exception. BS contributions (to the conventional SSPs) measured based on other MC star clusters are expected to be at a similar level as for ESO 121–SC03, and likely follow the same trend as for our previous results based on Galactic OCs covering a wide age range (Deng et al. 1999; XD05; XD07): the clusters’ age and/or metallicity estimates will be underestimated significantly, by a factor of 2–4, based on fits of SSPs to either spectra or broad-band colours. In a subsequent paper, we will discuss the equivalent results for the entire MC star cluster sample, i.e., based on the application of the method discussed here, which will significantly

**Table 2.** Fit Uncertainties for ESO 121-SC03

Real Parameter	SSP + All BSs		SSP + BSs ( $\leq R_{\text{HL}}$ )	
	Age = 8.9 Gyr	[Fe/H] = -0.97	Age = 8.9 Gyr	[Fe/H] = -0.97
Model Fit	3.4	-1.54	5.4	-1.28
Uncertainty (per cent)	62	59	40	32

extend the parameter coverage and the robustness of this conclusion.

In order to constrain the ISEDs of real stellar populations in a reliable way and to provide the community with a set of modified SSP models, extending our work on cluster samples to the MC rich star clusters is now in progress. In the context of our ultimate goal, we are currently still at the stage of information collection. To correct the conventional SSP models empirically, a sufficient working sample of clusters covering large ranges of age and metallicity, and of different dynamical environments, is definitely needed. Such a sample will provide statistical results of the BS contributions, and reliable information of BS populations in SSPs, such as the specific frequency of BSs (BS numbers in an SSP), and luminosity and colour functions of BSs (BS positions in a CMD). These will, we expect, eventually lead to the final solution to this problem, when we can construct the BS-corrected SSP models which can then be used in EPS studies in unresolved conditions.

## ACKNOWLEDGMENTS

YX, LD and ZH would like to thank the Chinese National Science Foundation for support through grants 10573022, 10778719, 10333060, 10521001, 10433030, and the Ministry of Science and Technology of China through grant 2007CB815406. YX acknowledges financial support from the Royal Society in the form of a ‘‘Sino-British Fellowship Trust Award’’. YX is also grateful to the International Astronomical Union for travel support from Beijing to the UK. RdG acknowledges partial funding from the Royal Society through an International Joint Project grant, as well as support for a high-level UK-China Science Network, funded by the Office of Science and Innovation of the UK government. ADM is supported by a Marie Curie Excellence Grant from the European Commission under contract MCEXT-CT-2005-025869.

This paper is based on observations made with the NASA/ESA *Hubble Space Telescope*, obtained at the Space Telescope Science Institute, which is operated by the Association of Universities for Research in Astronomy, Inc., under NASA contract NAS 5-26555. These observations are associated with programme #9891.

## REFERENCES

- Ahumada J.A., Lapasset E., 1995, *A&AS*, 109, 375  
Ahumada J.A., Lapasset E., 2007, *A&A*, 463, 789  
Alcaino G., Alvarado F., Borissova J., Kurtev R., 2003, *A&A*, 400, 917  
Bekki K., Beasley M.A., Forbes D.A., Couch W.J., 2004, *ApJ*, 602, 730  
Benz W., Hills J.G., 1987, *ApJ*, 323, 614  
Benz W., Hills J.G., 1992, *ApJ*, 389, 546  
Bertelli G., Bressan A., Chiosi C., Fagotto F., Nasi E., 1994, *A&AS*, 106, 275  
Bica E., Claria J.J., Dottori H., Santos Jr.J.F.C., Piatti A.E., 1996, *ApJS*, 102, 57  
Bica E., Geisler D., Dottori H., Claria J.J., Piatti A.E., Santos Jr.J.F.C., 1998, *AJ*, 116, 723  
Bruzual A. G., Charlot S., 2003, *MNRAS*, 344, 1000 (BC03)  
Burstein D., Heiles C., 1982, *AJ*, 87, 1165  
Carney B.W., Latham D.W., Laird J.B., 2005, *AJ*, 129, 466  
Da Costa G.S., 1991, in *IAU Symp. 148, The Magellanic Clouds*, Eds. Haynes R., Milne D., (Dordrecht: Kluwer), p183  
de Grijs R., Anders P., 2006, *MNRAS*, 366, 295  
Deng L., Chen R., Liu X.S., Chen J.S., 1999, *ApJ*, 524, 824  
Dirsch B., Richtler T., Gieren W.P., Hilker M., 2000, *A&A*, 360, 133  
Dolphin A.E., 2000, *PASP*, 112, 1383  
Ferraro F.R., Beccari G., Rood R.T., Bellazzini M., Sills A., Sabbi E., 2004, *ApJ*, 603, 127  
Ferraro F.R., Paltrinieri B., Fusi Pecci F., Cacciari C., Dorman B., Rood R.T., Buonanno R., Corsi C.E., Burgarella D., Laget M., 1997, *A&A*, 324, 915  
Ferraro F.R., Sills A., Rood R.T., Paltrinieri B., Buonanno R., 2003, *ApJ*, 588, 464  
Geisler D., Bica E., Dottori H., Clari J.J., Piatti A.E., Santos Jr.J.F.C., 1997, *AJ*, 114, 1920  
Girardi L., Bressan A., Bertelli G., Chiosi C., 2000, *A&AS*, 141, 371  
Gratton R.G., Bragaglia A., Carretta E., Clementini G., Desidera S., Grundahl F., Lucatello S., 2003, *A&A*, 408, 529  
Johnson J.A., Bolte M., Stetson P.B., Hesser J.E., Somerville R.S., 1999, *ApJ*, 527, 199  
Lanzoni B., Dalessandro E., Ferraro F.R., Mancini C., Beccari G., Rood R.T., Mapelli M., Sigurdsson S., 2007, *ApJ*, 663, 267  
Lee M.G., et al., 2003, *AJ*, 126, 2840  
Lejeune Th., Cuisinier F., Buser R., 1997, *A&AS*, 125, 229  
Liu G., Deng L., Chavez M.D., et al., 2008, in preparation  
Lombardi J.C.Jr., Rasio F.A., Shapiro S.L., 1995, *ApJ*, 445L, 117  
Lombardi J.C.Jr., Warren J.S., Rasio F.A., Sills A., Warren A.R., 2002, *ApJ*, 568, 939  
Mackey A.D., Broby Nielsen P., 2007, *MNRAS*, 379, 151  
Mackey A.D., Gilmore G.F., 2004, *MNRAS*, 352, 153  
Mackey A.D., Payne M.J., Gilmore G.F., 2006, *MNRAS*, 369, 921 (MPG06)  
Mackey A.D., Gilmore G.F., 2003a, *MNRAS*, 338, 85

- Mackey A.D., Gilmore G.F., 2003b, MNRAS, 338, 120  
Mapelli M., Ripamonti E., Tolstoy E., Sigurdsson S., Irwin M.J., Battaglia G., 2007, MNRAS, 380, 1127  
Mateo M., Hodge P., Schommer R.A., 1986, ApJ, 311, 113  
Mathys G., 1991, A&A, 245, 467  
Parmentier G., de Grijs R., 2007, MNRAS, accepted (arXiv:0710.3477)  
Piotto G., De Angeli F., King I.R., Djorgovski S.G., Bono G., Cassisi S., Meylan G., Recio-Blanco A., Rich R.M., Davies M.B., 2004, ApJ, 604, L109  
Protegiés Zwart S.F., Hut P., McMillan S.L.W., Verbunt F., 1997b, A&A, 328, 143  
Protegiés Zwart S.F., Hut P., Verbunt F., 1997a, A&A, 328, 130  
Sabbi E., Ferraro F.R., Sills A., Rood R.T., 2004, ApJ, 617, 1296  
Salpeter E.E., 1955, ApJ, 121, 161  
Sarajedini A., 1994, AJ, 107, 618  
Shetrone M.D., Sandquist E.L., 2000, AJ, 120, 1913  
Sills A., Adams T., Davies M.B., 2005, MNRAS, 358, 716  
Sills A., Pinsonneault M.H., Terndrup D.M., 2000, ApJ, 534, 335  
Sirianni M., et al., 2005, PASP, 117, 1049  
Tian B., Deng L., Han Z.W., Zhang X.B., 2006, A&A, 455, 247  
Warren S.R., Sandquist E.L., Bolte M., 2006, ApJ, 648, 1026  
Xin Y., Deng L., 2005, ApJ, 619, 824 (XD05)  
Xin Y., Deng L., Han Z.W., 2007, ApJ, 660, 319 (XDH07)

This paper has been typeset from a  $\text{\TeX}$ / $\text{\LaTeX}$  file prepared by the author.